Mixed Finite Element Methods as Finite Difference Methods for Solving Elliptic Equations on Triangular Elements

Todd Arbogast
Clint Dawson
Phil Keenan

November 1993

TR93-53

MIXED FINITE ELEMENTS AS FINITE DIFFERENCES FOR ELLIPTIC EQUATIONS ON TRIANGULAR ELEMENTS*

TODD ARBOGAST†, CLINT N. DAWSON†, AND PHILIP T. KEENAN†

Abstract. Five procedures of mixed finite element type for solving elliptic partial differential equations on triangular meshes are presented: the standard and hybrid mixed methods, the recently introduced expanded mixed method, and two new methods. The efficient implementation of these procedures using the lowest-order Raviart-Thomas approximating spaces defined on triangular elements is discussed. The standard method yields a saddle-point linear system, and while the hybrid method yields a positive definite linear system, it uses 50% more unknowns. A quadrature rule is given which reduces a new, expanded formulation of the mixed method to a finite difference method on triangles. This approach substantially reduces the complexity of the mixed finite element matrix. On smooth meshes this new approach appears to be as accurate as the standard method; on non-smooth meshes it can lose accuracy. An enhancement of this method is derived which combines numerical quadrature with Lagrange multipliers on certain element edges. The enhanced method regains the accuracy of the solution, with little additional cost if the mesh geometry is piece-wise smooth, as in hierarchical meshes. Numerical examples in two dimensions are given comparing the accuracy of the methods.

Keywords: Mixed finite element method, elliptic partial differential equation, finite differences, triangles

AMS(MOS) subject classification: 65N30, 65N06, 65N22

1. Introduction. In this paper, we discuss several variations of the mixed finite element method for solving elliptic equations of the form

$$-\nabla \cdot (K(\mathbf{x})\nabla p(\mathbf{x})) = f(\mathbf{x}), \quad \mathbf{x} \in \Omega, \tag{1}$$

where Ω is a polygonal domain in $\mathbb{R}^2$, $K(\mathbf{x})$ is a positive definite matrix, and for simplicity, we assume the boundary condition

$$p(\mathbf{x}) = 0, \quad \mathbf{x} \in \partial\Omega. \tag{2}$$

We concentrate on the efficient solution of (1) and (2) using the lowest-order Raviart-Thomas approximating spaces (RT_0) on triangular elements in two dimensions.

The mixed method (MM) was first described in [19]. The method has seen increasing popularity and an extensive literature has developed. The MM is especially useful for problems where the velocity or strain $\mathbf{u} = -K\nabla p$ is an important quantity, since, in general, mixed methods approximate $\mathbf{u}$ and the potential p to the same order of accuracy. Furthermore, the approximate velocity calculated by the mixed method satisfies the conservation principle $\nabla \cdot \mathbf{u} = f$ almost everywhere. This property is important in applications where local conservation of mass is essential.

General convergence properties of the MM are now well-understood. Convergence and superconvergence estimates can be found, for example, in [19, 8, 16, 23, 10, 11]. Since the standard MM yields a linear system that represents a saddle-point problem, much current research on the MM involves how to efficiently solve the system of equations that arises, see for example, [13, 5, 6, 12, 21, 17, 1].

Perhaps the earliest successful technique was the hybrid form of the mixed method (HM) [3]. This turns the saddle-point problem into a semi-definite problem, but at the expense of greatly increasing the number of unknowns.

* This research was supported in part by the Department of Energy, the State of Texas Governor's Energy Office, and project grants from the National Science Foundation. The third author was supported in part by an NSF Postdoctoral Fellowship.

† Department of Computational and Applied Mathematics, Rice University, P.O. Box 1892, Houston, TX 77251-1892.

Our primary interest in the MM is for solving elliptic and parabolic equations arising in flow through porous media, in particular, oil reservoir simulation and contaminant transport. In oil reservoir simulation, mixed finite element methods disguised as cell-centered finite difference methods have been the standard approach for many years [18]. The relationship between the mixed method and cell-centered finite differences was established in [20], under the assumption that K in (1) is a scalar or a diagonal matrix. If one uses the RT_0 approximating spaces on rectangular elements and applies appropriate quadrature rules, the mixed method reduces to a five-point cell-centered finite difference method for the potential p. Based on this observation, Weiser and Wheeler [23] were able to analyze and prove superconvergence for the potential and velocity approximations generated by this method. The resulting matrix problem is definite and generally much easier to solve than the problem which arises using the standard mixed method without quadrature.

Recently, a variation of the mixed method [1, 2] has been developed which has advantages over the standard approach for tensor and positive semi-definite coefficients K. In this method, an auxiliary variable is introduced to avoid inverting K, allowing K to be nonnegative — the standard mixed method assumes K is strictly positive. This expanded mixed method has the additional advantage over the MM that numerical quadrature can be used on rectangular meshes to derive a finite difference stencil even when K is a matrix function. We refer to this approach as the AWYM (Arbogast-Wheeler-Yotov method); convergence and superconvergence results are given in [1, 2].

In this paper, we derive a quadrature rule for triangular elements which reduces the expanded mixed method to a finite difference method for potential. In two dimensions, the finite difference stencil has ten points. As we demonstrate by example, the method is easy to solve and is as accurate as the MM, provided that the triangulation is "smooth". However, applying the quadrature rule on general triangulations can in some cases lead to an undesirable loss of accuracy in the solution. The loss of accuracy is caused by discontinuities in a mapping function which depends on the computational domain and the elements used in the triangulation. In cases where smooth triangulations can be used, the discontinuities disappear and no loss of accuracy occurs. Nevertheless, our ideas are useful for nonsmooth meshes for two reasons. First, the method can be used as a preconditioner for the MM or the AWYM without quadrature. Second, the loss of accuracy can be avoided by enhancing the method with Lagrange multipliers on element faces where the discontinuities appear.

The rest of this paper is outlined as follows. In the next Section, we give notation used throughout the paper. For completeness, we review the basic MM [19] in Section 3, the HM [3, 4] in Section 4, and the AWYM [1, 2] in Section 5. After this introductory material, we define the "cell-centered stencil method" (SM) in Section 6, which is the triangular analog of the AWYM. It is useful for smoothly triangulated domains. In Section 7, we work out an example to show why the SM can lose accuracy on nonsmooth meshes. In Section 8, we define the "enhanced cell-centered stencil method" (ESM), useful for triangulations consisting of the union of a small number of smooth triangulations. The ESM is a combination of the SM and the HM; it appears to give the same accuracy as HM with potentially much less computational cost. Finally, in Section 9, we present several numerical examples comparing the MM, HM, SM, and ESM. We also discuss briefly problems in three space dimensions. A C++ package which implements all of the methods presented here has been developed by the third author. More information on this package can be found in [14].

2. Notation. Let $L^2(R)$ denote the standard Sobolev space of square-integrable functions g on a domain $R \in \mathbb{R}^2$. We denote by $(\cdot,\cdot)_R$ the $L^2(R)$ inner product, and the $L^2(R)$ norm is denoted by

$$||g||_R = (g,g)_R^{\frac{1}{2}}. \tag{3}$$

Denote by $\langle\cdot,\cdot\rangle_{\partial R}$ the $L^2(\partial R)$ inner product. Define

$$H(\mathrm{div};R) = \{\mathbf{u} = (u^1,u^2) : \mathbf{u} \in (L^2(R))^2 \text{ and } \nabla\cdot\mathbf{u} \in L^2(R)\}, \tag{4}$$

with norm

$$||\mathbf{u}||^2_{H(\mathrm{div};R)} = \int_R \left[|\mathbf{u}|^2 + |\nabla\cdot\mathbf{u}|^2\right] d\mathbf{x}. \tag{5}$$

When $R = \Omega$, we may omit it in the definitions above.

Let $\mathcal{T}_h$ denote a triangulation of Ω into triangles with maximum diameter $h > 0$. Associated with $\mathcal{T}_h$, the RT_0 spaces $V_h \subset H(\mathrm{div};\Omega)$ and $W_h \subset L^2(\Omega)$ are characterized as follows [19]. Let N_T denote the number of triangles in $\mathcal{T}_h$ and N_e the number of edges. Then

$$W_h = \mathrm{span}\{w_i, i = 1,\ldots,N_T : (w_i)|_{T_j} = \delta_{ij}, j = 1,\ldots,N_T\}.$$

Letting $\mathbf{n}_\ell$ denote one of the unit vectors normal to edge ℓ, denoted by e_ℓ,

$$\begin{aligned} V_h = \mathrm{span}\{&\mathbf{v}_k \in H(\mathrm{div};\Omega), \quad k = 1,\ldots,N_e : \\ &\mathbf{v}_k|_T \in (\mathcal{P}^0(T))^2 \oplus \mathbf{x}\mathcal{P}^0(T) \quad \text{for all } T \in \mathcal{T}_h, \text{ and} \\ &\mathbf{v}_k\cdot\mathbf{n}_\ell|_{e_\ell} = \delta_{k\ell}, \quad \ell = 1,\ldots,N_e\}, \end{aligned}$$

where $\mathcal{P}^0(T)$ denotes the set of constant functions defined on $T \in \mathcal{T}_h$. Specifically, in $\mathbb{R}^2$, the function $\mathbf{v}_k = (v_k^1, v_k^2) \in V_h$ is given on T by

$$\begin{aligned} (v_k^1)|_T &= \alpha_T^1 + \beta x, \\ (v_k^2)|_T &= \alpha_T^2 + \beta y, \end{aligned}$$

with the three coefficients determined by the requirements

$$\mathbf{v}_k\cdot\mathbf{n}_\ell|_{e_\ell} = \delta_{k\ell}. \tag{6}$$

Thus $\mathbf{v}_k$ is nonzero only on the two elements which share edge k.

3. The Standard Mixed Method. To derive the MM[19], we rewrite (1) in mixed form:

$$\mathbf{u}(\mathbf{x}) = -K(\mathbf{x})\nabla p(\mathbf{x}), \tag{7}$$

$$\nabla\cdot\mathbf{u} = f. \tag{8}$$

Multiplying (7)–(8) by appropriate test functions and integrating we obtain

$$(K^{-1}\mathbf{u},\mathbf{v}) - (p,\nabla\cdot\mathbf{v}) = 0, \quad \mathbf{v} \in H(\mathrm{div};\Omega), \tag{9}$$

$$(\nabla\cdot\mathbf{u},w) = (f,w), \quad w \in L^2(\Omega). \tag{10}$$

In the MM, we seek $\mathbf{U} \in V_h$ and $P \in W_h$ that satisfy

$$(K^{-1}\mathbf{U}, \mathbf{v}) - (P, \nabla \cdot \mathbf{v}) = 0, \quad \mathbf{v} \in V_h, \tag{11}$$

$$(\nabla \cdot \mathbf{U}, w) = (f, w), \quad w \in W_h. \tag{12}$$

Define matrices M and B by

$$M_{ij} = (K^{-1}\mathbf{v}_j, \mathbf{v}_i), \quad i, j = 1, \ldots, N_e, \tag{13}$$

$$B_{ij} = (w_j, \nabla \cdot \mathbf{v}_i), \quad i = 1, \ldots, N_e; \quad j = 1, \ldots, N_T, \tag{14}$$

and vectors $\bar{\mathbf{U}}$, $\bar{P}$, and F by

$$\mathbf{U}(\mathbf{x}) = \sum_{j=1}^{N_e} \bar{\mathbf{U}}_j \mathbf{v}_j(\mathbf{x}), \tag{15}$$

$$P(\mathbf{x}) = \sum_{i=1}^{N_T} \bar{P}_i w_i(\mathbf{x}), \tag{16}$$

$$F_j = (f, w_j), \quad j = 1, \ldots, N_T. \tag{17}$$

Then $\mathbf{U}$ and P can be found by solving the matrix equation

$$\begin{bmatrix} M & -B \\ B^T & 0 \end{bmatrix} \begin{bmatrix} \bar{\mathbf{U}} \\ \bar{P} \end{bmatrix} = \begin{bmatrix} 0 \\ F \end{bmatrix}. \tag{18}$$

Existence and uniqueness of $\bar{\mathbf{U}}$ and $\bar{P}$ follows from our assumption of Dirichlet boundary conditions on p and the fact that M is positive definite, since (18) can be rewritten as

$$\bar{\mathbf{U}} = (M^{-1}B)\bar{P}, \tag{19}$$

$$A_{\mathrm{MM}}\bar{P} \equiv (B^T M^{-1} B)\bar{P} = F, \tag{20}$$

where $A_{\mathrm{MM}} = B^T M^{-1} B$ is symmetric and positive definite.

If exact integration is used in (13), then M is a sparse matrix but M^{-1} is full. When using an iterative method such as conjugate gradient iteration to solve (20), applying the matrix A_{MM} to a vector implies solving a system of equations involving the matrix M. As mentioned in the Introduction, in the special case of rectangular elements and K a scalar or a diagonal matrix function, then applying the appropriate quadrature rules to (13) reduces M and M^{-1} to diagonal matrices without reducing the accuracy of the approximate solutions [23]. In particular, assuming K is scalar,

$$(K^{-1}\mathbf{v}_j, \mathbf{v}_i) = (K^{-1}v_j^1, v_i^1) + (K^{-1}v_j^2, v_i^2), \tag{21}$$

and we can approximate the first integral on the right side using the trapezoidal rule in x and the midpoint rule in y, using the reverse rules for the second integral. The matrix A_{MM} then becomes sparse with nonzero entries on five bands, and the cost of applying an iterative procedure to the solution of (20) is greatly reduced. In fact, the method reduces to the standard cell-centered finite difference method.

It was proven in [19] that for $\mathbf{u}$ and p sufficiently smooth, the RT_0 approximations $\mathbf{U}$ and P satisfy

$$||\mathbf{u} - \mathbf{U}||_{H(\mathrm{div};\Omega)} + ||P - p|| \le Ch, \tag{22}$$

where C is a constant independent of h. For rectangular meshes and K a scalar or diagonal matrix, superconvergence of order h^2 of the velocity $\mathbf{U}$ and potential P at Gauss points was proven in [16]. These results were extended in [10] to demonstrate superconvergence of velocities along lines connecting Gauss points. In [23], these results were shown to hold even when numerical quadrature of the type discussed above is used to approximate the integral $(K^{-1}\mathbf{v}_j, \mathbf{v}_i)$. On triangular meshes, superconvergence of the potential P of order h^2 at the centroid of each triangle was proven in [11, 8]. No superconvergence results for velocity are known in this case. Our numerical results seem to indicate that the velocity is not superconvergent on triangular meshes.

4. The Hybrid Method. Next, we consider a hybrid version of the MM (HM) [3], where Lagrange multipliers are introduced on the element edges. We modify the RT_0 spaces slightly, introducing spaces V_h' and Λ_h, with V_h' replacing V_h. For each triangle $T \in \mathcal{T}_h$ with edges e_k, k=1,2,3, we associate basis functions $\mathbf{v}_{T,k}$ that satisfy $\mathbf{v}_{T,k} \in (\mathcal{P}^0(T))^2 \oplus \mathbf{x}\mathcal{P}^0(T)$ and $\mathbf{v}_{T,k} \cdot \mathbf{n}_l = \delta_{k,l}$, where $\mathbf{n}_l$ is the unit outward normal (with respect to T) to edge e_l. The space $V_h' \subset (L^2(\Omega))^2$ is given by

$$V_h' = \text{span}\{\mathbf{v}_{T,k}, k = 1, 2, 3,\ T \in \mathcal{T}_h\};$$

it is V_h with relaxed continuity requirements. Let E denote the union of all element edges in $\mathcal{T}_h$. The space $\Lambda_h \subset L^2(E)$ is given by

$$\Lambda_h = \text{span}\{\mu_j, j = 1, \ldots, N_e : \mu_j = 1 \text{ on edge } j \text{ and } 0 \text{ elsewhere}\}. \tag{23}$$

Let $\Lambda_h^0 = \Lambda_h \cap \{v : v = 0 \text{ on } \partial\Omega\}$.

Returning to (7)–(8), multiplying by appropriate test functions and integrating, we find

$$(K^{-1}\mathbf{u}, \mathbf{v}) = (p, \nabla \cdot \mathbf{v}) - \sum_{T \in \mathcal{T}_h} \langle p, \mathbf{v} \cdot \mathbf{n}_T \rangle_{\partial T}, \quad \mathbf{v} \in (L^2(\Omega))^2, \tag{24}$$

$$(\nabla \cdot \mathbf{u}, w) = (f, w), \quad w \in L^2(\Omega). \tag{25}$$

In (24), $\mathbf{n}_T$ represents the unit outward normal to ∂T. Approximate $\mathbf{u}$ by $\mathbf{U} \in V_h'$, p in each element T by $P \in W_h$, and p on ∂T by $\lambda \in \Lambda_h^0$. The unknowns $\mathbf{U}$, P, and λ satisfy

$$(K^{-1}\mathbf{U}, \mathbf{v}) = (P, \nabla \cdot \mathbf{v}) - \sum_{T \in \mathcal{T}_h} \langle \lambda, \mathbf{v} \cdot \mathbf{n}_T \rangle_{\partial T}, \quad \mathbf{v} \in V_h', \tag{26}$$

$$(\nabla \cdot \mathbf{U}, w) = (f, w), \quad w \in W_h, \tag{27}$$

$$\sum_{T \in \mathcal{T}_h} \langle \mathbf{U} \cdot \mathbf{n}_T, \mu \rangle_{\partial T} = 0, \quad \mu \in \Lambda_h^0. \tag{28}$$

It is easily shown that (26)–(28) is equivalent to the MM; that is, $\mathbf{U} \in V_h$, and $\mathbf{U}$ and P satisfy (11)–(12). Thus, the convergence and superconvergence of the HM follows from the analysis for the MM.

The computational difference between (26)–(28) and (11)–(12) is that one can solve directly for λ, and then compute $\mathbf{U}$ and P. Let $\bar{\mathbf{U}}$, $\bar{P}$, and $\bar{\lambda}$ denote the vectors of unknowns associated with the functions $\mathbf{U}$, P, and λ, respectively. In matrix form, (26)–(28) can be written as

$$\begin{bmatrix} \bar{M} & -\bar{B} & L \\ \bar{B}^T & 0 & 0 \\ L^T & 0 & 0 \end{bmatrix} \begin{bmatrix} \bar{\mathbf{U}} \\ \bar{P} \\ \bar{\lambda} \end{bmatrix} = \begin{bmatrix} 0 \\ F \\ 0 \end{bmatrix}. \tag{29}$$

This system can be reduced to an equation for $\bar{\lambda}$ as follows. The first equation in (29) gives

$$\bar{\mathbf{U}} = \bar{M}^{-1}(\bar{B}\bar{P} - L\bar{\lambda}). \tag{30}$$

From the second equation equation and (30)

$$\bar{B}^T\bar{\mathbf{U}} = \bar{B}^T\bar{M}^{-1}(\bar{B}\bar{P} - L\bar{\lambda}) = F; \tag{31}$$

thus,

$$\bar{P} = \left(\bar{B}^T\bar{M}^{-1}\bar{B}\right)^{-1}\left(F + \bar{B}^T\bar{M}^{-1}L\bar{\lambda}\right). \tag{32}$$

Let $A_1^{-1} = \bar{B}^T\bar{M}^{-1}\bar{B}$. Finally, from the third equation, (30), and (32), we find

$$[L^T\bar{M}^{-1}\bar{B}A_1\bar{B}^T\bar{M}^{-1}L - L^T\bar{M}^{-1}L]\bar{\lambda} = -(L^T\bar{M}^{-1}\bar{B}A_1)F. \tag{33}$$

Let A_{HM} denote the matrix on the left side of (33).

The matrix $\bar{M}$ is block diagonal; each block corresponds to one triangle in $\mathcal{T}_h$, and is a symmetric, positive definite, 3×3 matrix. Hence $\bar{M}^{-1}$ is also block diagonal and easy to compute. The matrix $\bar{B}^T\bar{M}^{-1}\bar{B}$ has the same structure, so A_1 is also block diagonal. Furthermore, L has at most two nonzero entries on any row or column; thus, A_{HM} can be formed and is sparse, with at most five nonzero entries on any row. The stencil for λ is given in Figure 1. Hence, the advantage of solving (33) over (20) for triangular meshes is that the matrix A_{HM} is easier to apply than A_{MM}. The disadvantage is that (33) involves 50% more unknowns than (20), and in three dimensions, this ratio is 2:1 for tetrahedra and 3:1 for bricks.

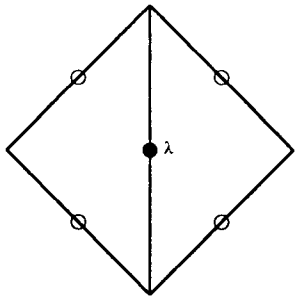

FIG. 1. *Stencil for λ for the HM*

5. The AWY Expanded Mixed Method. In this section, we present the Arbogast-Wheeler-Yotov variation of the MM [1, 2]. We introduce a mesh-dependent function S_g, which we define explicitly below. For now, assume S_g is a symmetric, positive definite, 2×2 matrix function. We also introduce an auxiliary variable $\mathbf{y}$, defined by

$$S_g\mathbf{y} = -\nabla p; \tag{34}$$

then

$$S_g\mathbf{u} = S_gKS_g\mathbf{y}. \tag{35}$$

If $S_g(\mathbf{x})$ is invertible, (34)–(35) is equivalent to (7). With (8), a corresponding weak form is given by

$$(S_g\mathbf{y},\mathbf{v}) = (p,\nabla\cdot\mathbf{v}), \quad \mathbf{v}\in H(\mathrm{div};\Omega), \tag{36}$$

$$(S_g\mathbf{u},\mathbf{z}) = (S_gKS_g\mathbf{y},\mathbf{z}), \quad \mathbf{z}\in (L^2(\Omega))^2, \tag{37}$$

$$(\nabla\cdot\mathbf{u},w) = (f,w), \quad w\in L^2(\Omega). \tag{38}$$

Let T denote any triangle in $\mathcal{T}_h$, and let T_{ref} denote a reference element, which we assume is the equilateral triangle with vertices at $(-1,0)$, $(1,0)$, and $(0,\sqrt{3})$. Let D_T denote the constant Jacobian matrix of the affine mapping between element T and T_{ref}, and let $J_T = |\det D_T|$. On each element T in $\mathcal{T}_h$, define S_g by

$$S_g|_T = J_T(D_T)^T D_T. \tag{39}$$

Note that S_g on each element is indeed symmetric and positive definite. We approximate $\mathbf{y}$ by $\mathbf{Y}\in V_h$, $\mathbf{u}$ by $\mathbf{U}\in V_h$, and p by $P\in W_h$, where $\mathbf{Y}$, $\mathbf{U}$, and P satisfy

$$(S_g\mathbf{Y},\mathbf{v}) = (P,\nabla\cdot\mathbf{v}), \quad \mathbf{v}\in V_h, \tag{40}$$

$$(S_g\mathbf{U},\mathbf{z}) = (S_gKS_g\mathbf{Y},\mathbf{z}), \quad \mathbf{z}\in V_h, \tag{41}$$

$$(\nabla\cdot\mathbf{U},w) = (f,w), \quad w\in W_h. \tag{42}$$

Introduce the matrices S and C defined by

$$S_{ij} = (S_g\mathbf{v}_j,\mathbf{v}_i), \quad i,j=1,\ldots,N_e, \tag{43}$$

$$C_{ij} = (S_gKS_g\mathbf{v}_j,\mathbf{v}_i), \quad i,j,=1,\ldots,N_e, \tag{44}$$

and define B as before in (14). Let $\bar{\mathbf{Y}}$, $\bar{\mathbf{U}}$, and $\bar{P}$ be the vectors of unknowns associated with $\mathbf{Y}$, $\mathbf{U}$, and P, respectively. Then $\bar{\mathbf{Y}}$, $\bar{\mathbf{U}}$, and $\bar{P}$ satisfy

$$\begin{bmatrix} S & 0 & -B \\ C & -S & 0 \\ 0 & B^T & 0 \end{bmatrix} \begin{bmatrix} \bar{\mathbf{Y}} \\ \bar{\mathbf{U}} \\ \bar{P} \end{bmatrix} = \begin{bmatrix} 0 \\ 0 \\ F \end{bmatrix}. \tag{45}$$

In this case, S and C are symmetric, positive definite, and sparse, and (45) implies

$$\bar{\mathbf{Y}} = S^{-1}B\bar{P}, \tag{46}$$

$$\bar{\mathbf{U}} = S^{-1}CS^{-1}B\bar{P}, \tag{47}$$

$$A_{\mathrm{AWYM}}\bar{P} \equiv \left(B^TS^{-1}CS^{-1}B\right)\bar{P} = F. \tag{48}$$

The matrix $A_{\mathrm{AWYM}} = B^TS^{-1}CS^{-1}B$ is symmetric and positive definite; hence, $\bar{P}$ exists and is unique, and the existence and uniqueness of $\bar{\mathbf{U}}$ and $\bar{\mathbf{Y}}$ follow from (47) and (46).

One advantage of the AWYM over the MM is that the weak form (36)–(38) does not require calculating K^{-1} as in (9)–(10). Thus, the AWYM is definable in cases where $K(\mathbf{x}) = 0$. For time-dependent problems where K may vary with time, the AWYM also has the advantage over the MM that only S^{-1} is needed in the computation, not M^{-1}. Unlike M, S is not time-dependent and hence S^{-1} can be calculated once at the beginning of the computation, whereas M^{-1} must be recomputed each time-step.

In general, the computational expense of the AWYM and the MM are roughly equivalent, since S^{-1} and M^{-1} are both full matrices. In the case of rectangular

elements, however, we can choose $S_g \equiv I$, the identity matrix, and the integrals in (43) can be approximated by quadrature rules as in the MM, reducing S to a diagonal matrix [1]. Thus, like A_{MM}, A_{AWYM} becomes a sparse, banded matrix. Another advantage of the AWYM over the MM is that this reduction can be applied even when K is a matrix function, since K does not enter into the computation of S. This reduction is especially useful, for example, in transport equations where K represents a diffusion-dispersion tensor.

The convergence theory for the AWYM is given in [1, 2], where it is shown that pressure and velocity are globally first order accurate, and pressures are superconvergent at the center of mass of each element, provided that S_g varies smoothly over the domain. In our case, S_g is piecewise discontinuous, so this convergence theory does not apply directly.

6. The Stencil Method on triangles. As noted above, applying the AWYM or the MM on general triangulations gives matrices which are expensive to apply. In this section, we describe a method for approximating the integrals in (43) on triangular meshes which diagonalizes the matrix S. The result is a sparse approximation to A_{AWYM} that in two space dimensions has at most ten nonzero entries on any given row. We refer to this approach as the Cell-Centered Stencil Method, or SM.

On any triangle T, let $\mathbf{v}_k$ denote the basis function of V_h associated with edge k, denoted by e_k, $k = 1, 2, 3$. On T_{ref}, let $\hat{e}_k$ denote the edge which is the image of e_k when T is mapped to T_{ref}. Define the Piola transformation [22] for vectors by

$$\hat{\mathbf{v}}_k = J_T D_T \mathbf{v}_k, \quad k = 1, 2, 3. \tag{49}$$

It can then be verified that

$$\int_T (S_g \mathbf{v}_k) \cdot \mathbf{v}_l \, d\mathbf{x} = \int_{T_{\mathrm{ref}}} \hat{\mathbf{v}}_k \cdot \hat{\mathbf{v}}_l \, d\mathbf{x}, \tag{50}$$

for $k, l = 1, 2, 3$. Moreover, from (49), one can show that $\hat{\mathbf{v}}_k$ is a scalar multiple of the standard basis function for V_h corresponding to edge k of T_{ref}. Thus,

$$\hat{\mathbf{v}}_k \cdot \hat{\mathbf{n}}_l = \alpha_k \delta_{kl}, \quad k, l = 1, 2, 3, \tag{51}$$

where $\hat{\mathbf{n}}_l$ is the normal to edge l on T_{ref}, and α_k is a scale factor,

$$\alpha_k = \frac{\text{length } e_k}{\text{length } \hat{e}_k}. \tag{52}$$

In order to diagonalize the matrix S, we seek a quadrature rule which diagonalizes (50). We define a quadrature rule $Q_T(g)$ on T_{ref} such that $Q_T(g)$ is exact for polynomials of degree one, and $Q_T(\hat{\mathbf{v}}_k \cdot \hat{\mathbf{v}}_l) = 0$ for $k \neq l$:

$$Q_T(g) = \frac{\sqrt{3}}{6}\left[g(-1,0) + g(1,0) + g(0,\sqrt{3}) + 3g\left(0, \frac{\sqrt{3}}{3}\right)\right]. \tag{53}$$

Thus, by (50),

$$\int_T (S_g \mathbf{v}_k) \cdot \mathbf{v}_l \, d\mathbf{x} \approx Q_T(\hat{\mathbf{v}}_k \cdot \hat{\mathbf{v}}_l) = \begin{cases} 0, & k \neq l, \\ \frac{\sqrt{3}}{6}(\text{ length } e_k)^2, & k = l. \end{cases} \tag{54}$$

Let S_D denote the diagonal approximation to S determined by the quadrature rule given above. Define

$$A_{\mathrm{SM}} = B^T S_D^{-1} C S_D^{-1} B. \tag{55}$$

Then A_{SM} is a sparse approximation to A_{AWYM}. The resulting stencil for P is given in Figure 2. In particular, on any row of A_{SM}, there are at most ten nonzero entries.

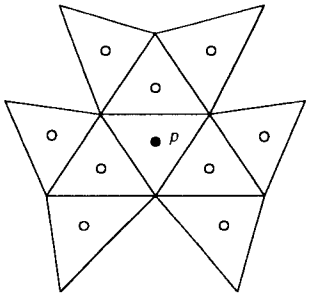

FIG. 2. *Stencil for P for the SM*

The approach described above can easily be extended to three space dimensions, using a similar quadrature rule. In this case, A_{SM} has at most seventeen nonzero entries.

7. A Non-smooth Mesh Example. In this section we discuss mesh smoothness and refinement processes and their impact on the accuracy of the SM. We say that a mesh is *smooth* if it is the image under a smooth map f of a mesh of equilateral triangles. Of course, any mesh can be called smooth under this definition by making f have large derivatives. The cost is that the constant in convergence rates will depend on the derivatives of f. We say a mesh refinement process (as used in a convergence study, for instance) is *smooth* if it can be carried out by uniformly refining the mesh of equilateral triangles and taking the image under the same f. A mesh refinement process is called *hierarchical* if an initial coarse mesh is refined using a smooth refinement process inside each of the original coarse elements.

In practice, most applications use meshes and refinement schemes which can be classified as smooth or hierarchical. The numerical experiments in Section 9 show that on smooth meshes, the SM is as accurate as the MM. As this section will illustrate, the accuracy of the SM can be impared by using non-smooth meshes. Section 8 will define an Enhanced Stencil Method which corrects this problem efficiently for hierarchical mesh refinement processes.

Consider the two triangle mesh shown in Figure 3. Using Dirichlet boundary conditions and taking the true solution $p = y$, one can work out the computed solution P and $\mathbf{U}$ by hand. The usual mixed method would reproduce the linear P and constant $\mathbf{U}$ exactly. The SM, in contrast, fails to compute either correctly; for instance it yields $P = 0.35714$ for the pressure at the centroids of the triangles, instead of 0.33333. If uniform refinement is applied to this mesh, the errors converge much more slowly than with the MM.

Figure 4 shows the error $P - p$ when p is a linear function, on a much finer mesh constructed from applying uniform refinement to an original coarse mesh of 2 non-similar triangles. Darker shades indicate larger errors. Within each of the original

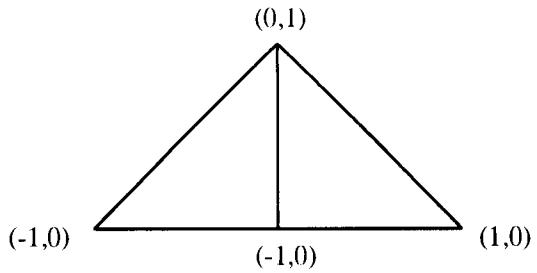

FIG. 3. *A non-smooth mesh.*

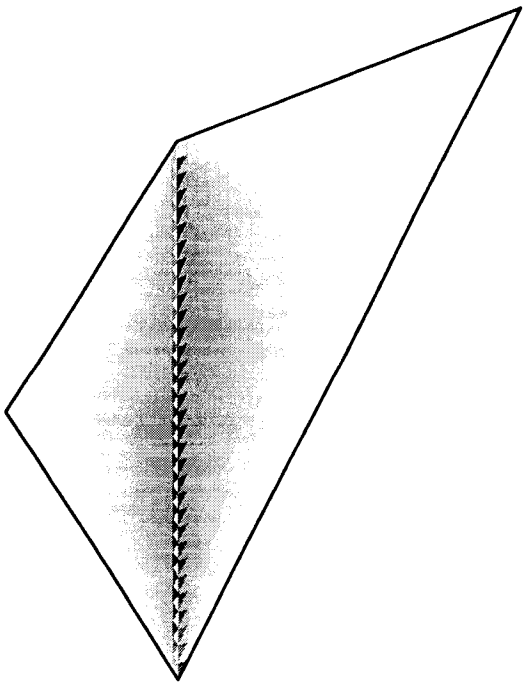

FIG. 4. *Error in $P - p$ on a hierarchically refined mesh using the SM*

triangles the mesh is smooth; the jump in S_g across the central line produces the error pattern shown, somewhat like an artificial source term.

The problem is that $\mathbf{y} = S_g^{-1}\nabla p$ is discontinuous across faces where S_g changes discontinuously, but it is approximated by a function $\mathbf{Y} \in V_h$ which is constrained to have continuous normal components across faces. This suggests that adding Lagrange multipliers to such faces, thereby enriching the discrete space in which Y is defined, should solve the problem. The ESM of Section 8 does precisely this, and can be shown to solve the two element problem of Figure 3 exactly in the case of linear p.

8. The Enhanced Stencil Method. In this section, we discuss the Enhanced Cell-Centered Stencil Method (ESM), which is a combination of the SM with Lagrange multipliers added at edges where S_g is not smooth.

In the HM, Lagrange multipliers were introduced on the boundary of every element in $\mathcal{T}_h$. In some cases, Lagrange multipliers are only needed on the boundaries of a few elements. For example, when applying the domain decomposition techniques described in [13], Lagrange multipliers are introduced only on the element edges where subdomains intersect. In this method, just as in (33), one can reduce the global system of equations to an equation for the Lagrange multipliers. Applying the resulting matrix operator involves solving subdomain problems for velocity and potential. In this section, we follow a similar approach, introducing Lagrange multipliers only on certain element edges. This defines the Enhanced Cell-Centered Stencil Method. In this case, the multipliers are needed to preserve accuracy of the numerical solution; however, as a side effect, they can be used to introduce parallelism into the solution process as well.

In order to describe the basic idea, consider a domain Ω consisting of two regions Ω_1 and Ω_2 separated by an interface Γ, such as that given in Figure 5. Assume a triangulation of Ω is constructed, where S_g is smooth in Ω_1 and Ω_2 but not necessarily smooth along Γ. In Ω_1 and Ω_2 we will apply the SM as described above. The two subdomains will be coupled by Lagrange multipliers along the edge Γ.

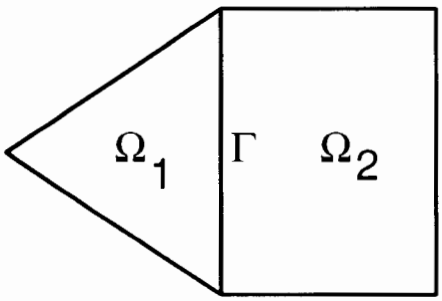

FIG. 5. *Domain decomposition*

Let $\mathcal{T}_h^k$ denote a triangulation of Ω_k, $k = 1, 2$, and $\mathcal{T}_h = \mathcal{T}_h^1 \cup \mathcal{T}_h^2$. We assume the triangulations $\mathcal{T}_h^1$ and $\mathcal{T}_h^2$ match at the edge Γ, so that $\mathcal{T}_h$ is a valid triangulation of the whole domain Ω. Let $V_h^k \subset H(\mathrm{div};\Omega_k)$, $W_h^k \subset L^2(\Omega_k)$ denote the RT_0 spaces on $\mathcal{T}_h^k$, k=1,2. Let $V_h^* = V_h^1 \cup V_h^2$, and $W_h = W_h^1 \cup W_h^2$. Let $\Lambda_h^* \in L^2(\Gamma)$ denote the restriction to Γ of the space Λ_h defined in (23).

Returning to (34)–(35), (38), multiplying by appropriate test functions and inte-

grating, we obtain

$$(56)\quad (S_g\mathbf{y},\mathbf{v}) = (p,\nabla\cdot\mathbf{v}) - \sum_{k=1}^{2}\langle p,\mathbf{v}\cdot\mathbf{n}_k\rangle_\Gamma, \quad \mathbf{v}\in H(\mathrm{div};\Omega_1)\cup H(\mathrm{div};\Omega_2),$$

where $\mathbf{n}_k$ is the outward normal to $\partial\Omega_k\cap\Gamma$, $k=1,2$,

$$(57)\quad (S_g\mathbf{u},\mathbf{z}) = (S_gKS_g\mathbf{y},\mathbf{z}), \quad \mathbf{z}\in(L^2(\Omega))^2,$$

$$(58)\quad (\nabla\cdot\mathbf{u},w) = (f,w), \quad w\in L^2(\Omega).$$

Let $\mathbf{Y},\mathbf{U}\in V_h^*$, $P\in W_h$, and $\lambda\in\Lambda_h^*$, where $\mathbf{Y}$, $\mathbf{U}$, P, and λ approximate $\mathbf{y}$, $\mathbf{u}$, p, and $p|_\Gamma$, respectively, and satisfy

$$(59)\quad (S_g\mathbf{Y},\mathbf{v}) = (P,\nabla\cdot\mathbf{v}) - \sum_{k=1}^{2}\langle\lambda,\mathbf{v}\cdot\mathbf{n}_k\rangle_\Gamma, \quad \mathbf{v}\in V_h^*,$$

$$(60)\quad (S_g\mathbf{U},\mathbf{z}) = (S_gKS_g\mathbf{Y},\mathbf{z}), \quad \mathbf{z}\in V_h^*,$$

$$(61)\quad (\nabla\cdot\mathbf{U},w) = (f,w), \quad w\in W_h,$$

$$(62)\quad \sum_{k=1}^{2}\langle\mathbf{U}\cdot\mathbf{n}_k,\mu\rangle_\Gamma = 0, \quad \mu\in\Lambda_h^*.$$

We approximate the left-most terms in (59) and (60) using the quadrature rule (54).

In matrix form, (59)–(62) (with quadrature) can be written as

$$(63)\quad \begin{bmatrix} \tilde{S}_D & 0 & -\tilde{B} & \tilde{L} \\ \tilde{C} & -\tilde{S}_D & 0 & 0 \\ 0 & \tilde{B}^T & 0 & 0 \\ 0 & \tilde{L}^T & 0 & 0 \end{bmatrix} \begin{bmatrix} \bar{\mathbf{Y}} \\ \bar{\mathbf{U}} \\ \bar{P} \\ \bar{\lambda} \end{bmatrix} = \begin{bmatrix} 0 \\ 0 \\ F \\ 0 \end{bmatrix}.$$

This system can be reduced to a system for $\bar{P}$ and $\bar{\lambda}$ as follows. From the first equation,

$$(64)\quad \bar{\mathbf{Y}} = \tilde{S}_D^{-1}(\tilde{B}\bar{P} - \tilde{L}\bar{\lambda}).$$

From the second equation and (64),

$$(65)\quad \bar{\mathbf{U}} = \tilde{S}_D^{-1}\tilde{C}\tilde{S}_D^{-1}(\tilde{B}\bar{P} - \tilde{L}\bar{\lambda}).$$

Let $A_2 = \tilde{S}_D^{-1}\tilde{C}\tilde{S}_D^{-1}$. From the third equation and (65),

$$(66)\quad \tilde{B}^T\bar{\mathbf{U}} = (\tilde{B}^TA_2\tilde{B})\bar{P} - (\tilde{B}^TA_2\tilde{L})\bar{\lambda} = F,$$

and from the fourth equation and (65),

$$(67)\quad -\tilde{L}^T\bar{\mathbf{U}} = -(\tilde{L}^TA_2\tilde{B})\bar{P} + (\tilde{L}^TA_2\tilde{L})\bar{\lambda} = 0.$$

Thus we obtain the system

$$(68)\quad \begin{bmatrix} A_3 & D \\ D^T & A_4 \end{bmatrix} \begin{bmatrix} \bar{P} \\ \bar{\lambda} \end{bmatrix} = \begin{bmatrix} F \\ 0 \end{bmatrix},$$

where $A_3 = \tilde{B}^T A_2 \tilde{B}$, $A_4 = \tilde{L}^T A_2 \tilde{L}$, and $D = -\tilde{B}^T A_2 \tilde{L}$. Denote the matrix on the left side of (68) by A_{ESM}. If desired, (68) can be further reduced to an equation for $\bar{\lambda}$ alone, in particular,

$$\bar{P} = A_3^{-1}(F - D\bar{\lambda}), \tag{69}$$

and

$$(A_4 - D^T A_3^{-1} D)\bar{\lambda} = -D^T A_3^{-1} F. \tag{70}$$

In [13, 5, 12, 6], various methods for solving (70) on parallel computers are developed and analyzed. In all of these approaches, applying the matrix on the left side of (70) involves solving a problem of the form

$$A_3 x = b \tag{71}$$

for some vector x and right hand side b. The matrix A_3 decouples across subdomains, thus (71) involves independent subdomain problems which can be solved simultaneously.

The matrices A_3, D, and A_4 can be formed and easily applied to vectors. In particular, the ESM can be thought of in a domain decomposition setting as introducing Lagrange multipliers on subdomain boundaries, then using the SM within each subdomain. However, we require more generality. In particular, we introduce Lagrange multipliers across any edge where S_g is discontinuous. Depending on the geometry of the domain and the type of triangulation used, this may result in introducing a substantial number of Lagrange multipliers. However, for domains which can be divided into a relatively small number of regular domains, where uniform triangulations can be used, the ESM should be roughly as efficient as the SM.

9. Numerical results. We created a large suite of test problems which we used to examine the behavior of the numerical methods described above. We varied the shape of the domain, the coefficient tensor K, and the analytic solution. In each case the boundary conditions and the forcing term were constructed to match the prescribed solution. We report in detail on two typical cases and then summarize the results from the full test suite.

9.1. Two Typical Cases. Among the domains considered were those shown in Figures 6 and 7. These figures illustrate the initial decomposition of the domains into elements. The second domain is neither simply connected nor convex; moreover we chose to use both rectangles and triangles in subdividing it, to illustrate the flexibility of the C++ program.

In the convergence study, the smooth example domain was described by cubic splines, which were used to generate progressively finer meshes directly. The resulting family of meshes meets the definition of smooth given in Section 7.

In contrast, the non-smooth example domain was refined uniformly to generate progressively finer meshes. Each application of uniform refinement replaced each triangle or rectangle with 4 smaller but geometrically similar ones. The finest mesh had 2432 elements. Uniform refinement generates hierarchical meshes: each new mesh contains all the edges of the previous one. However, discontinuities in the geometry mapping across edges of the original coarse triangulation are not smoothed out by refinement. Thus this family of meshes is hierarchical but not smooth, as defined in Section 7.

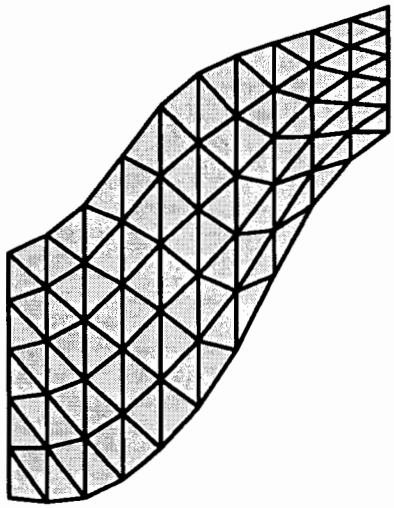

FIG. 6. *Smooth Mesh Example*

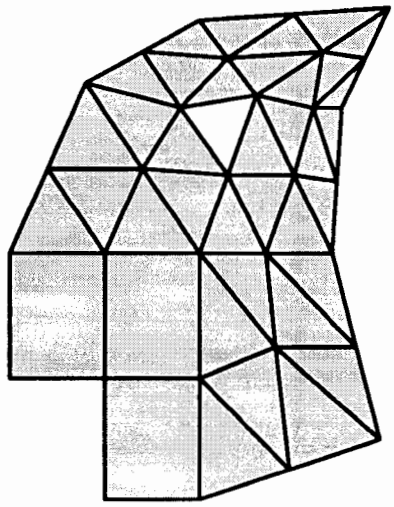

FIG. 7. *Non-smooth Mesh Example*

In Tables 1–4, we give detailed results on both domains for a test problem using Dirichlet boundary conditions,

$$K = \begin{pmatrix} 1 & 0.5 \\ 0.5 & 3 \end{pmatrix},$$

and with the analytic solution

$$p(x,y) = 1.2x^3 + 2.1x^2y + 3.1xy^2 - 4.1y^3 - 1.1x^2 + 2.4xy + 1.7y^2 + 2x - 3y + 1.$$

We report the l^2 norm of the error in the pressure p and the flux $K\nabla p$. The l^2 norm is the discrete two-norm taken at the centers of elements. The error in the flux refers to the flux as a vector, not to just one component. As can be seen in Tables 1 and 2, the MM, HM, and SM are equally accurate for the smooth example. The nonsmooth, hierarchical example of Tables 3 and 4, however, shows that the SM loses accuracy (about one half power of h) in both p and $-K\nabla p$, as compared to the MM and HM. However, the ESM is as accurate as the MM and HM in all the examples.

h	**MM = HM**	**SM**
0.01	0.010	0.0064
0.0025	0.0027	0.0015
0.0006	0.00068	0.00037
Rate	h^2	h^2

TABLE 1
l^2 error in p for the smooth example

h	**MM = HM**	**SM**
0.01	0.62	0.63
0.0025	0.32	0.32
0.0006	0.16	0.16
Rate	h	h

TABLE 2
l^2 error in $K\nabla p$ for the smooth example

h	**MM = HM**	**SM**	**ESM**
0.16	0.39	0.48	0.59
0.08	0.11	0.12	0.11
0.04	0.029	0.043	0.026
0.02	0.0076	0.019	0.0062
Rate	h^2	$h^{1.4}$	h^2

TABLE 3
l^2 error in p for the non-smooth example

h	MM = HM	SM	ESM
0.16	6.0	9.3	6.4
0.08	3.1	5.9	3.5
0.04	1.5	3.7	1.6
0.02	0.77	2.5	0.80
Rate	h	$h^{0.6}$	h

TABLE 4
l^2 error in $K\nabla p$ for the non-smooth example

9.2. Tetrahedra. The C++ program can handle three dimensional elements such as bricks and tetrahedra. We observed numerically that the stencil approach breaks down on tetrahedral meshes. This appears to be due to the fact that regular tetrahedra do not fill space, whereas equilateral triangles do tile the plane. This means that the geometry matrix S_g is unavoidably discontinuous everywhere, no matter how much one attempts to smooth the tetrahedral mesh. Therefore, the HM seems to be the best choice for tetrahedral meshes. The SM could, however, be used with prismatic elements on meshes constructed from the tensor product of a triangular mesh in two dimensions and a one dimensional collection of intervals.

9.3. Summary. We conducted approximately 100 experiments varying the domain, the shape of the elements, the type of mesh refinement used, the test equation, and the tensor K.

For most methods and test cases, the condition number of the linear system was $O(h^{-1})$, as estimated by the number of conjugate gradient iterations used. However, the ESM combined with uniform refinement produced better conditioned systems, with condition numbers around $O(h^{-0.9})$. Using a conjugate gradient solver with no preconditioning, the MM took much longer than the other three methods (approximately 50 times longer on 2000 elements). On a typical smooth mesh problem the SM took approximately half as much CPU time as the HM. The ESM was somewhat slower than the HM on coarse meshes, since it solves for both pressures and Lagrange multipliers. By around four levels of mesh refinement it had caught up to the HM, since it did not need Lagrange multipliers on every edge, and it should outperform it when additional refinement is used.

The error in the pressure converged approximately like $O(h^2)$ for the MM, HM, SM, and ESM, except that the SM converged at a slower rate for hierarchical meshes; that is, in non-smooth situations, where the geometry matrix changes discontinuously because of uniform refinement. Similarly the error in the flux converged like $O(h)$, except for SM with geometry discontinuities. Using smooth refinement on the non-smooth domain illustrated above in Figure 7, the SM achieved the same convergence orders as the other methods.

On rectangles one finds that the velocities are superconvergent at special points and can be post-processed to yield second order accurate vector approximations everywhere. A new post processing scheme developed by the third author recovers extra accuracy for the velocities on triangular meshes as well [15]. The postprocessing method can be applied to any of the mixed method variants. The convergence rate for the post processed flux is generally between $h^{1.5}$ and $h^{1.9}$, depending in part on the smoothness of the mesh refinement process. This and other related postprocessing schemes are analyzed in [9], where it is shown that they recover second order accurate velocity fields on three-lines meshes. Moreover, although the resulting ve-

locity fields do not conserve mass exactly, a special postprocessor choice makes the mass conservation errors extra small.

10. Conclusions. The SM has been seen to be an accurate and efficient method for smooth meshes of triangular elements, that appears to be about twice as fast as competing methods. On hierarchical meshes, the SM loses accuracy, but the ESM does not. The ESM can be more efficient than the HM if the coarse elements are sufficiently refined that the ESM requires many fewer Lagrange multiplier unknowns than the HM. On meshes of tetrahedral elements, however, the SM loses accuracy, so the HM should be used instead.

REFERENCES

[1] T. Arbogast, M. F. Wheeler, and I. Yotov, *Mixed Finite Elements for Elliptic Problems with Tensor Coefficients as Finite Differences.* Technical Report TR94-02, Department of Computational and Applied Mathematics, Rice University, 1994.

[2] T. Arbogast, M. F. Wheeler, and I. Yotov, *Mixed finite element methods on general geometry.* (in preparation).

[3] D. N. Arnold, and F. Brezzi, *Mixed and nonconforming finite element methods: implementation, postprocessing and error estimates.* Modélisation Mathématiques et Analyse Numérique 19, pp. 7–32, 1985.

[4] F. Brezzi and M. Fortin, *Mixed and hybrid finite elements*, Springer Series in Computational Mathematics, Vol. 15, Springer-Verlag, Berlin, 1991.

[5] L. C. Cowsar, M. F. Wheeler, and J. Mandel, *Balancing domain decomposition for cell-centered finite differences*, to appear.

[6] L. C. Cowsar, A. Weiser, and M. F. Wheeler, *Parallel multigrid and domain decomposition algorithms for elliptic equations*, Fifth International Symposium on Domain Decomposition Methods for Partial Differential Equations, D. Keyes, T. F. Chan, G. Meurant, J. S. Scroggs, R. G. Voigt, eds., SIAM, Philadelphia, pp. 376-385, 1992.

[7] J. Douglas, Jr., R. E. Ewing, and M. F. Wheeler, *Approximation of the pressure by a mixed method in the simulation of miscible displacement*, RAIR Model. Math. Anal., Numer., 17, pp. 17-33, 1983.

[8] J. Douglas, Jr., and J.E. Roberts, *Global estimates for mixed methods for second order elliptic equations*, Math. Comp., 44, pp. 39–52, 1985.

[9] T. F. Dupont, and P. T. Keenan, *Postprocessing mixed method velocities on triangular elements.* Technical Report, Department of Computational and Applied Mathematics, Rice University,(in preparation).

[10] R. E. Ewing, R. D. Lazarov, and J. Wang, *Superconvergence of the velocity along the Gauss lines in mixed finite element methods*, SIAM J. Numer. Anal., **28**, pp. 1015-1029, 1991.

[11] L. Gastaldi and R. Nochetto, *Optimal L^∞-error estimates for nonconforming and mixed finite element methods of lowest order*, Numer. Math., **50**, pp. 587-611, 1987.

[12] R. Glowinski, W. Kinton, and M. F. Wheeler, *Acceleration of domain decomposition algorithms for mixed finite elements by multi-level methods*, in Third International Symposium on Domain Decomposition Methods for Partial Differential Equations, T. F. Chan, R. Glowinski, J. Periaux, O. Widlund, eds., SIAM, Philadelphia, pp. 263-289, 1990.

[13] R. Glowinski and M. F. Wheeler, *Domain decomposition and mixed finite element methods for elliptic problems*, in First International Symposium on Domain Decomposition Methods for Partial Differential Equations, R. Glowinski, G. H. Golub, G. Meurant, J. Periaux, eds., SIAM, Philadelphia, pp. 144-172, 1988.

[14] P. Keenan, *Instructions for my C++ elliptic PDE solver programs using mixed methods on general geometries*, Technical Report TR93-56, Department of Computational and Applied Mathematics, Rice University, 1993.

[15] P. T. Keenan, *An efficient postprocessor for velocities from mixed methods on triangular elements.* Technical Report, Department of Computational and Applied Mathematics, Rice University,(in preparation).

[16] M. Nakata, A. Weiser, and M. F. Wheeler, *Some superconvergence results for mixed finite element methods for elliptic problems on rectangular domains*, in The Mathematics of Finite Elements and Applications V, J. R. Whiteman, ed., Academic Press, London, 1985.

[17] V. J. Parr, *Preconditioner schemes for elliptic saddle-point matrices based upon Jacobi multi-band polynomial matricies*, Ph.D. Thesis, Dept. of Comp. and Appl. Math., Rice University, in preparation.

[18] D. W. Peaceman, *Fundamentals of numerical reservoir simulation*, Elsevier, Amsterdam, 1977.

[19] P. A. Raviart and J. M. Thomas, *A mixed finite element method for 2nd order elliptic problems*, in Mathematical Aspects of the Finite Element Method, Lecture Notes in Math., Springer-Verlag, Berlin, 1977.

[20] T. F. Russell and M. F. Wheeler, *Finite element and finite difference methods for continuous flows in porous media*, in The Mathematics of Reservoir Simulation, R. E. Ewing, ed., SIAM, 1983.

[21] T. Rusten, *Iterative methods for mixed finite element systems*, Ph.D. Thesis, Dept. of Informatics, University of Oslo, 1991.

[22] J.M. Thomas, *These de Doctorat d'etat à l'Universite Pierre et Marie Curie*, 1977.

[23] A. Weiser and M. F. Wheeler, *On convergence of block-centered finite differences for elliptic problems*, SIAM J. Numer. Anal., **25**, pp. 351-375, 1988..